

Ultra Low-Power Photovoltaic MPPT Technique for Indoor and Outdoor Wireless Sensor Nodes

Alex S. Weddell, Geoff V. Merrett, Bashir M. Al-Hashimi

School of Electronics and Computer Science, University of Southampton, SO17 1BJ, UK

{asw,gvm,bmah}@ecs.soton.ac.uk

Abstract—Photovoltaic (PV) energy harvesting is commonly used to power wireless sensor nodes. To optimise harvesting efficiency, maximum power point tracking (MPPT) techniques are often used. Recently-reported techniques focus solely on outdoor applications, being too power-hungry for use under indoor lighting. Additionally, some techniques have required light sensors (or pilot cells) to control their operating point. This paper describes an ultra low-power MPPT technique which is based on a novel system design and sample-and-hold arrangement, which enables MPPT across the range of light intensities found indoors and outdoors and is capable of cold-starting. The proposed sample-and-hold based technique has been validated through a prototype system. Its performance compares favourably against state-of-the-art systems, and does not require an additional pilot cell or photodiode. This represents an important contribution, in particular for sensors which may be exposed to different types of lighting (such as body-worn or mobile sensors).

I. INTRODUCTION

Recent advances in energy harvesting and storage technologies [1] now mean that wireless sensor nodes can be designed to operate indefinitely from energy ‘harvested’ from their environment. A common form of energy harvesting technology is from light by means of photovoltaic (PV) modules, but these usually require Maximum Power Point Tracking (MPPT) circuitry in order to adjust the operating point of the cell in response to changing light conditions and maintain its operation at the Maximum Power Point (MPP).

A number of techniques are available to realise MPPT with PV cells. The established techniques are ‘hill-climbing’ and ‘fractional open-circuit voltage’ (FOCV) [2]. In the case of the hill-climbing method, the operating point of the PV cell is continually modified; if the modification results in an increase in the power obtained from the cell, the operating point will continue to be adjusted in the same direction (conversely, for a drop in generated power, the operating point will then be modified in the opposite direction). While this method ensures that the PV module operates at its MPP, it is only suitable for outdoor applications as it requires fine-grained control of the system, normally necessitating the use of a microcontroller.

The FOCV technique exploits the property that the MPP voltage of some PV cells is proportional to their open-circuit voltage. The techniques vary for realising this method, but generally they rely on the periodic disconnection of the PV module in order that its open-circuit voltage may be sampled, or the system may use additional light sensors as a proxy to

determine the MPPT voltage of the cell. Conventional systems for FOCV-based MPPT in outdoor applications have been described, for example by Enslin *et al.* [3], which samples the PV module twice per minute (but was intended for very large panels, so the quiescent power consumption can be assumed to be high), and [4] which samples the module every 100ms (and has an overall power consumption of $\approx 2\text{mW}$). Existing state-of-the-art small systems (i.e. with small PV cells but designed for outdoor use) have used a ‘pilot’ solar cell [5] (for which the overall system consumes $\approx 300\mu\text{W}$ when ‘off’) or photodetector [6] (which consumes $\approx 500\mu\text{A}$) to control the operating point of the module.

The low light intensities experienced indoors mean that maximum power point tracking (MPPT) circuitry designed for outdoor use is too power-hungry to operate indoors (indoor PV cells typically produce $\ll 1\text{mW}$). Hence, state-of-the-art works for indoor PV-harvesting either ignore MPPT completely [7] (a valid assumption for cases where the energy store voltage is always sufficiently close to the MPP voltage of the PV module), or operate the PV cell at a fixed voltage which is assumed to be sufficiently close to the MPP voltage [8].

This paper considers scenarios where sensors powered from PV cells may be expected to experience a mix of both natural and artificial lighting (for example mobile devices or body-worn sensors). The justification for this work is in realising an MPPT circuit which, due to its simplified and efficient operation, is able to operate under a range of lighting conditions. While the proposed technique has been prototyped and tested with PV modules, it is also applicable to other forms of energy harvesting (such as thermoelectric generators) which feature a similar relationship between the open-circuit and MPP voltage [9]. The proposed system advances the state-of-the-art through the following novel contributions:

- An ultra-low-power MPPT system that can cold start and operate in a very wide range of lighting conditions including the low intensities found indoors.
- A sample-and-hold system which accurately samples the open-circuit voltage of the PV cell, holds this value for extended periods, and draws an average $8\mu\text{A}$.

II. PV PROPERTIES AND SAMPLING

A. Cell properties

Amorphous silicon (a-Si) PV cells have a relatively high efficiency at low light levels, compared to other types of

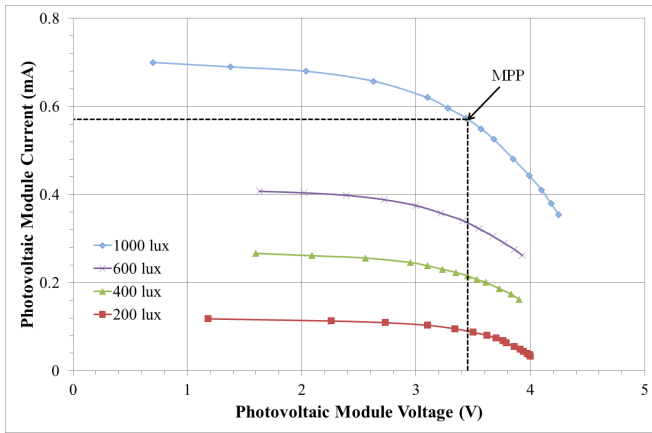


Fig. 1. I-V curve of Schott Solar 1116929 amorphous silicon PV cell under artificial light. Dashed line indicates location of MPP at 1000 lux. Derived from experimental data.

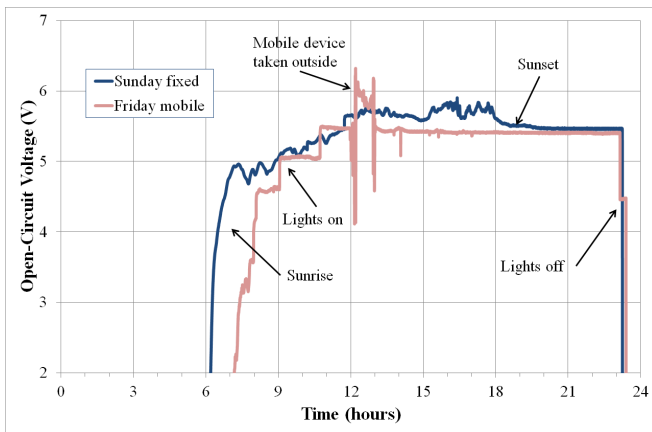


Fig. 2. 24-hour log of open-circuit voltage of PV cell, with cell placed on an office desk. The desk is lit by a mix of artificial and natural light. Sunrise, and lights-off at the end of the day, can easily be identified.

cell. This makes them particularly suited to use indoors. An additional feature of amorphous silicon (and, indeed, all non-crystalline) PV cells is that their MPP voltage (V_{mpp}) is approximately proportional to their open-circuit voltage (V_{oc}). As shown in (1), the proportion is expressed by parameter k . This relationship is exploited by some MPP circuits, which periodically sample the open-circuit voltage of the PV cell in order to decide its activity level.

$$V_{mpp} \approx k \cdot V_{oc} \quad (1)$$

The parameter k is typically between 0.6 and 0.8, and depends mainly on the chemistry of the cell. As stated by [10], there is also a weak correlation between k and the light intensity. The relationship is only ever an approximation to the MPP, but is easily realised in hardware and does not rely on active monitoring of the cell performance (as is required for the hill-climbing MPPT method).

B. Sampling parameters

As the proposed circuit periodically samples the open-circuit voltage of the PV module, it was necessary to assess the dynamics of indoor and outdoor light levels to decide on an appropriate sampling rate. Tests of the open-circuit voltage of the module were carried out over a 24-hour period, as shown in Fig. 2; two tests were carried out, the first being on a lab desk on a Sunday (with the blinds closed); the other was in a lab on a Friday, with the cell being taken outdoors at lunchtime (this mimics the light conditions to which a mobile sensor may be exposed).

The collected data have been analyzed in order to assist with the selection of an appropriate sampling frequency for the system. The method shown in (2) was used to calculate the worst-case mean error for the estimate of open-circuit voltage that would result from a certain sampling frequency. Here, \bar{E} is the mean error, n is the counting variable, p is the period between each sample, and q is the test duration.

$$\bar{E} = \sum_{q-p}^{n=0} \frac{\max \{x_n \dots x_{n+p-1}\} - \min \{x_n \dots x_{n+p-1}\}}{q-p+1} \quad (2)$$

This has been used to calculate the mean error in the estimate of open-circuit voltage, assuming that a discrete test is taken once per time interval. For a 1-minute hold period with the 24-hour test data, the worst-case mean error has also been calculated. The desk-mounted 24-hour test shows that a 1-minute period gives $\bar{E} = 12.7\text{mV}$, and the 1-day semi-mobile test gives $\bar{E} = 24.1\text{mV}$. These equate to errors in the estimate of MPP voltage of approximately 7.7mV and 14.7mV respectively. Taking the worst error calculated for the MPP voltage and mapping this across to the performance curve for an amorphous silicon PV module (shown in Fig. 1), this equates to an efficiency loss of less than 1%. Therefore, a long hold period (of $>60\text{s}$) is justified for the design of MPPT circuits which use this technique.

III. DEMONSTRATOR DEVELOPMENT

A. Overall system operation

Cold starting is enabled through a small capacitor; once this has been charged to a sufficient level and a threshold voltage has been reached, the MPPT circuit is switched on. The MPPT then controls the other switches on the circuit, periodically sampling the open-circuit voltage of the PV cell (by way of an ultra low-power sample-and-hold arrangement) and thus controlling the voltage at which the switching converter operates. This arrangement delivers effective cold-start operation, and the complete metrology circuit is potentially very low-power. The form of MPPT chosen, FOCV, requires periodic sampling of the open-circuit voltage of the PV cell. The parameters of these sampling operations are important, as they require the cell to be disconnected from the load (and therefore must be minimized).

The system is comprised of three major interlinked modules, as shown in Fig. 3. The figure shows the interconnection

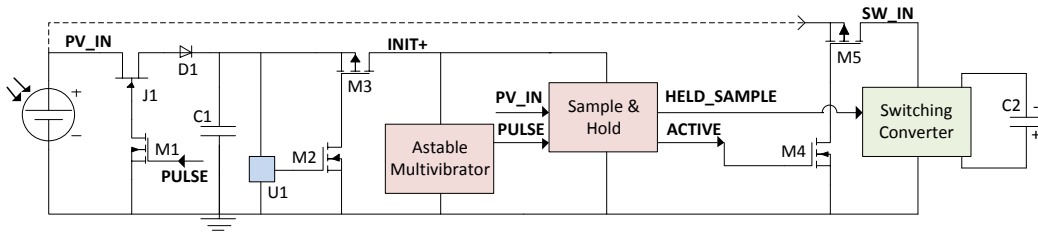


Fig. 3. Simplified overall system platform

between these modules, and illustrates how they interact and how cold-start operation and periodic sampling is achieved. As a brief overview, the astable generates pulses of a certain duration and frequency, which triggers samples of the PV V_{oc} . The sample-and-hold circuit takes these measurements and ‘holds’ them. A switching converter has been developed, which is based on the circuit presented in [8] and consists of a modified buck-boost converter. During normal operation, this circuit acts to maintain a constant voltage across its input terminals in order to keep the PV module at a voltage indicated by HELD_SAMPLE. The PV module is maintained at this fixed voltage, which is provided by the HELD_SAMPLE line from the sample-and-hold circuit. It was designed and optimised in line with earlier reported works such as [5], [8] but was forced to use an alternative PV cell model as described in Sec. II. The additional circuitry is to facilitate the cold-start of the system and to allow measurements of the V_{oc} to be taken. The components used in this system were selected for their low on-resistance for relatively small gate voltages in order to maximise the efficiency of the system.

B. Sample-and-hold arrangement

The sample-and-hold arrangement, which incorporates the astable multivibrator and the sample-and-hold circuits, provides three outputs to the rest of the system: firstly, the PULSE output acts to initiate a sample of the voltage across the PV module, disconnecting all loads from the PV module’s output. The HELD_SAMPLE output is a fraction of the open-circuit voltage of the PV module. The equation for HELD_SAMPLE is shown by (3), where k is the fixed ratio between V_{oc} and V_{mpp} (typically between 0.6 and 0.8), and η is the proportion by which this is reduced for representation by the circuit.

$$\text{HELD_SAMPLE} = V_{oc} \cdot k \cdot \eta \quad (3)$$

The astable multivibrator circuit arrangement is adapted from the square-wave generator circuit in [11], and is comprised of a micropower comparator (National Semiconductor LMC7215) and passive components including a low-leakage polyester capacitor. The period of the high and low signals can be independently adjusted.

The sample-and-hold circuit is enabled through the use of an analog switch, a low-leakage sampling capacitor, and a unity gain buffer at the input and output of the circuit. The system relies on two op-amps to realise the input (U2) and output



Fig. 4. Sampling operation taking place at 1000 lux. Shows the PULSE line which disconnects all loads from the solar cell and modifies the HELD_SAMPLE line. A small ripple may be observed when the test is being carried out.

(U4) unity gain buffers. The ACTIVE output is provided by comparator U5, which compares the HELD_SAMPLE output against an arbitrary threshold voltage provided by dividing the supply rail voltage by two. This serves as a sanity check to ensure that the switching converter will not try to start until a valid voltage is held. MOSFET M8 acts to pull the IN+ terminal down when sampling operations are taking place, which ensures that the switching converter is also disabled.

IV. EXPERIMENTAL DATA

A. System Testing

The operation of the system has been verified in a range of tests. Fig. 4 shows detail of a sampling operation, in which the PV cell’s open-circuit voltage is disconnected from its load and is used to update the HELD_SAMPLE output. A small ripple may be observed on the HELD_SAMPLE line, but its effect is mitigated by the combination of R3 and C3. The operating voltage of the PV cell has also been tested to ensure that it is consistent with the HELD_SAMPLE output.

The sample-and-hold circuit and astable multivibrator have been tested together, connected to a mains power supply in order that the operation could be verified and the current draw could be determined. The astable multivibrator produced an ‘on’ period of 39ms and an ‘off’ period of 69s. The current draw of the combination of the astable multivibrator and the sample-and-hold circuit was measured at an average of $7.6\mu\text{A}$

TABLE I
TEST OF TRACKING ACCURACY

Intens. (lux)	V_{oc} (V)	HELD (V)	k %	Intens. (lux)	V_{oc} (V)	HELD (V)	k %
200	4.978	1.483	59.6	800	5.369	1.596	59.5
300	5.096	1.513	59.4	900	5.41	1.609	59.5
400	5.18	1.542	59.5	1000	5.44	1.624	59.7
500	5.242	1.554	59.3	2000	5.64	1.674	59.4
600	5.292	1.566	59.2	3000	5.75	1.691	59.8
700	5.333	1.580	59.2	5000	5.91	1.775	60.1

at 3.3V. This compares favourably against the AM-1815 cell's MPP current and voltage of $42\mu\text{A}$ and 3.0V, meaning that at 200 lux <18% of the power obtained from the cell is used to power the sample-and-hold circuitry at this low intensity level. The AM-1815 cell has an area of only 25cm^2 [12].

The accuracy of the MPPT circuitry has been assessed by way of a sequence of tests at differing light intensities. As shown in Table I, the system was tested at a range of light intensities from 5,000 lux down to 200 lux (5,000 lux was the maximum intensity possible under the test set-up without causing excessive heating of the PV cell). The table presents the value of the open-circuit voltage and of the HELD_SAMPLE line, along with the calculated value of k that this equates to. The circuitry was tested as part of the complete system. Each test was repeated three times for each intensity level, and the mean of the three results is presented here. It may be observed that all values fall within the range 59.2% to 60.1%. This value may easily be trimmed by means of a variable potentiometer in place of R2 in order to bring it to any desired value of k (in the nominal range 0.6 to 0.8).

B. Evaluation

The proposed MPPT technique has been evaluated by way of a sequence of tests. The cold-start of the system has been observed down to light levels of 200 lux, with a SANYO Amorton AM-1815 cell (a smaller PV cell than that has been used in the earlier reported works). The additional current draw of the sample-and-hold circuitry is $8\mu\text{A}$, which is less than 20% of the current produced at 200 lux by the SANYO Amorton AM-1815 cell used to verify this work. In fact, the current draw of the sample and hold circuitry presented here (permitting MPPT) is less than that of a voltage reference IC used in the reported fixed-voltage technique [8].

The system has been shown to cold-start and quickly generate a signal on the PULSE line to initiate the first measurement of the open-circuit voltage. The system interfaces with the switching converter. While the design of the actual switching converter is not the main focus of this paper, the system's operation in combination with this switching converter has been validated. The tracking of the MPP has been shown to be consistent and can be trimmed using a variable potentiometer. With only one low on-resistance MOSFET in the line between the PV cell and the switching converter, it can be summarized that there is a negligible impact on the overall efficiency of the

system as a result of the new sample-and-hold and cold-start arrangement that has been presented.

V. CONCLUSION

This paper has presented a novel technique for realising an ultra low-power MPPT system that can be used both indoors and outdoors, and does not require additional light sensors or pilot cells. Systems had until now been designed either to operate indoors (in which case, MPPT is not attempted), or operate efficiently outdoors (in which case the tracking circuitry itself consumed all of the power generated indoors). The proposed technique has been evaluated by way of a prototype. With a quiescent current draw of $8\mu\text{A}$, the new sample-and-hold arrangement now permits MPPT to take place in applications where it was previously impractical. This is of particular interest for mobile and body-worn devices.

ACKNOWLEDGMENT

This work was supported in part by the Engineering and Physical Sciences Research Council (EPSRC) under grant number EP/G067740/1 "Next Generation Energy-Harvesting Electronics: Holistic Approach," website: www.holistic.ecs.soton.ac.uk

REFERENCES

- [1] S. Beeby and N. White, Eds., *Energy Harvesting for Autonomous Systems*. London, UK: Artech House, 2010.
- [2] T. Eswam and P. Chapman, "Comparison of photovoltaic array maximum power point tracking techniques," *Energy Conversion, IEEE Transactions on*, vol. 22, no. 2, pp. 439–449, 2007.
- [3] J. Enslin, M. Wolf, D. Snyman, and W. Swiegers, "Integrated photovoltaic maximum power point tracking converter," *Industrial Electronics, IEEE Transactions on*, vol. 44, no. 6, pp. 769–773, 1997.
- [4] F. Simjee and P. Chou, "Efficient charging of supercapacitors for extended lifetime of wireless sensor nodes," *Power Electronics, IEEE Transactions on*, vol. 23, no. 3, pp. 1526–1536, 2008.
- [5] D. Brunelli, L. Benini, C. Moser, and L. Thiele, "An efficient solar energy harvester for wireless sensor nodes," in *DATE '08: Proceedings of the conference on Design, automation and test in Europe*. New York, NY, USA: ACM, 2008, pp. 104–109.
- [6] C. Park and P. Chou, "Ambimax: Autonomous energy harvesting platform for multi-supply wireless sensor nodes," *Sensor and Ad Hoc Communications and Networks, 2006. SECON '06. 2006 3rd Annual IEEE Communications Society on*, vol. 1, pp. 168–177, 2006.
- [7] W. Wang, T. O'Donnell, L. Ribetto, B. O'Flynn, M. Hayes, and C. O'Mathuna, "Energy Harvesting Embedded Wireless Sensor System for Building Environment Applications," in *Proceedings of the International Conference on Wireless Communications, Vehicular Technology, Information Theory and Aerospace & Electronic Systems Technology, Wireless Vitae*, vol. 1, 2009, pp. 36–41.
- [8] A. S. Weddell, N. R. Harris, and N. M. White, "An efficient indoor photovoltaic power harvesting system for energy-aware wireless sensor nodes," in *EuroSensors 2008*, September 2008, pp. 1544–1547.
- [9] I. Laird, H. Lovatt, N. Savvides, D. Lu, and V. Agelidis, "Comparative study of maximum power point tracking algorithms for thermoelectric generators," *Power Engineering Conference, 2008. AUPEC '08. Australasian Universities*, pp. 1–6, 2008.
- [10] D. Brunelli, D. Dondi, A. Bertacchini, L. Larcher, P. Pavan, and L. Benini, "Photovoltaic scavenging systems: Modeling and optimization," *Microelectronics Journal*, vol. 40, no. 9, pp. 1337–1344, 2009.
- [11] National Semiconductor Corp., "LM6772 Data Sheet," 2010. [Online]. Available: <http://www.national.com/ds/LM/LMC6772.pdf>
- [12] SANYO Semiconductor Co., Ltd., "AM-1815 Data Sheet," 2008, last accessed Sept. 2010. [Online]. Available: <http://www.farnell.com/datasheets/87124.pdf>